Higgs dynamics in the early universe

Vis, J.M. van de

Chapter 7

The importance of leptons for electroweak baryogenesis

7.1 Introduction

We saw in the previous chapter that the baryon asymmetry from a dimension-six CPV top source is much smaller than the observed value of the baryon asymmetry. In this chapter we investigate why the top source is inefficient in generating the observed baryon asymmetry and explore the effects of including leptons.

We will use a relatively simple framework, inspired by effective field theory. The applicability of the SM-EFT is limited, as we saw in chapter 6, because new *light* degrees of freedom are necessary to obtain a strong first-order phase transition. In this chapter we mainly focus on the CPV dynamics and avoid the issue of the first-order phase transition by describing the bubble-wall profile in terms of the phenomenological tanh-function introduced in section 5.2.2.

As in chapter 6, we describe the required additional CPV by effective dimension-six CPV operators containing SM fields only. In principle the CPV dynamics could arise from effective operators involving any new fields that play a role in the phase transition [322], but as these are difficult to probe in experiments we ignore such interactions for now. In particular, we focus on effective dimension-six Yukawa interactions of various quarks and leptons as these are representative for popular classes of BSM models such as multi-Higgs models. Chapter 6 and similar studies in the literature have focussed on CPV in the top-quark sector [3, 278, 282], as the large top Yukawa coupling maximizes the CPV source term in the transport equations that describe the dynamics of the particle number densities. However, taking into account the most recent constraint on the

electric dipole moment of the electron [297], the 'top-source scenario' gives an asymmetry that is about two orders of magnitude too small to explain the baryon asymmetry [3].

The small value of the baryon asymmetry in the top-source scenario has prompted our current study of the general features of the solutions to the transport equations, to find ways to boost the asymmetry. The reasons for the inefficiency of the top-source scenario are threefold. First, the diffusion of the chiral asymmetry into the symmetric phase is not efficient for the strongly-interacting quarks [323]. Second, EDM measurements put strong constraints on CPV in the top sector [302] such that the strength of the CPV source term is limited. And third, the washout of the produced chiral asymmetry is significant for (top) quarks, as the top Yukawa and especially the strong sphaleron interactions effectively wash out the chiral asymmetry in the symmetric phase, except for regions very close to the bubble wall [314, 324]. These problems can potentially be overcome by looking at CPV source terms involving lighter fermions. For instance, EDM limits are less stringent for bottom quarks. While the CPV source term for bottom quarks is suppressed by the smaller Yukawa coupling, the washout rate due to Higgs interactions is suppressed accordingly. As such, the total baryon asymmetry is not a simple function of the size of the Yukawa coupling.

For leptons there can be even more advantages even though they have been neglected in many studies of EWBG. While the CPV source term is suppressed, leptons diffuse into the plasma much more easily [323], the EDM limits are less stringent for muon and tau CPV interactions [288], and the washout rate is less effective because leptons do not interact via strong sphalerons. Already in Refs. [273, 323, 325–327] the effect of leptons on EWBG was studied in a range of scenarios in which the lepton Yukawa coupling is enhanced significantly with respect to the SM values. We will show that even with the small SM Yukawa interactions, including leptons can dramatically change the baryon asymmetry in models with CPV source terms involving top quarks. In addition, we show that leptonic CPV source terms can be very efficient in producing the baryon asymmetry of the universe. Scenarios with a CPV leptonic source are also great diagnostic tools as the set of transport equations is relatively simple. We use this scenario to understand the parametric dependence of the baryon asymmetry on bubble wall parameters and the size of Yukawa couplings. This study confirms that the baryon asymmetry is not a simple function of the size of the Yukawa coupling. And while we focus on a particular set-up, the importance of leptons and the general mechanisms at play are more general.

As we will show, the role of leptons in EWBG depends on the effectiveness of the exchange of the chiral asymmetry between quarks and leptons. In the SM this exchange is not very efficient because of the small lepton Yukawa interactions. In various BSM models there can be more efficient

mechanisms, for example via the exchange of additional scalar fields. Such mechanisms can strongly boost the baryon asymmetry if the CPV source term is located in the quark sector by transferring the chiral asymmetry into the lepton sector, where it diffuses faster and suffers from less washout. Conversely, it can suppress the baryon asymmetry if the CPV source term is located in the lepton sector. We model this phenomenon by adding effective dimension-six quark-lepton interactions; this set-up qualitatively explains features of various models studied in recent literature [326, 327]. We also comment on the effect of possible new BSM quark-quark couplings, which may likewise boost the baryon asymmetry for a source located in the quark sector, as this coupling affects and limits the washout from strong sphaleron interactions.

This chapter is organized as follows. In the next section we introduce the set-up and briefly describe the first-order phase transition and bubble profile, the CPV dimension-six operators and the EDM and LHC constraints. We briefly touch upon the transport equations and the computation of the baryon asymmetry, but for the details we refer to sections 5.3, 5.4 and 5.5. We then identify the factors that suppress the value of the baryon asymmetry in the top-source scenario and motivate the importance of leptons. We also introduce a new top-lepton interaction. We start with a discussion of the tau-source scenario in section 7.3. The lepton sector almost completely decouples from the quark sector, and the baryon asymmetry can be computed analytically in this limit to good accuracy. We identify the important length scales, and discuss the physics and mechanisms at play. In section 7.4 we give the results for the top-source scenario. The equations to solve are more intricate, but the outcome can be understood qualitatively. We also comment on the viability of a bottom-source scenario and briefly discuss even lighter fermions. Finally, in section 7.5 we describe the effects of a new tau-top coupling on both the tau- and top-source scenario. We end with a discussion in section 7.6.

7.2 Set-up and methods

7.2.1 First-order phase transition

There are many BSM models that modify the Higgs sector such that the phase transition becomes first order. Well studied examples are the $\mathbb{Z}_2$-symmetric Higgs-singlet model [316–321] and two-Higgs doublet models [328–335]. In the previous chapter, we argued that a first-order electroweak phase transition cannot be described in a systematic EFT expansion and explicit light degrees of freedom

must be introduced. This unfortunately prohibits a model-independent approach, and it is necessary to pick a specific BSM model to implement the first-order phase transition.

Once a BSM model is chosen, one can solve the tunnelling equations of motion at the nucleation temperature T_N to find the so-called bounce solution φ_b [245]. We parameterize the Higgs doublet as $\Phi = (\Phi^+, \Phi^0)^T$ and in the bubble background $\langle \Phi^0 \rangle = \frac{1}{\sqrt{2}} \varphi_b(z)$. In this chapter, we will use the parametrization of eq. (5.15), which provides a reasonable description of the bubble-wall profile in many models. More complicated profiles can be studied in similar fashion. We do not expect our findings in this chapter to change significantly if more complicated profiles are applied. As in chapters 5 and 6 we use the planar wall approximation, in which curvature effects are neglected. Further, $v_N = v(T_N)$ is the vacuum expectation value of the Higgs field in the broken phase at the nucleation temperature T_N, and L_w the bubble width. In principle, these parameters should be determined by fitting the bounce solution of a BSM model to eq. (5.15). However, our prime interest is not the phase transition itself but the comparison of different sources of CP violation. We work with benchmark parameters $T_N = 88\,\text{GeV}$, $v_N = 152\,\text{GeV}$, and $L_w = 0.11\,\text{GeV}^{-1}$. For the velocity of the bubble wall we take the benchmark value $v_w = 0.05$. We will investigate how the produced asymmetry depends on these parameters.

7.2.2 Source of CP violation

We use the same CPV operator as in scenario **A** of chapter 6, but now also allow for CP-violation for lighter quarks and leptons. That is, we assume that apart from a modified scalar sector that ensures a first-order phase transition, other BSM degrees of freedom are sufficiently heavy and can be integrated out leading to effective operators. We consider the flavor-diagonal CPV dimension-six operators

$$\mathcal{L}_6 = -i \left[\bar{Q}_L \tilde{Y}_U \tilde{\Phi}\, u_R \;+\; \bar{Q}_L \tilde{Y}_D \Phi\, d_R \;+\; \bar{L}_L \tilde{Y}_L \Phi\, e_R \right] (\Phi^\dagger \Phi) + \text{h.c.}\,, \tag{7.1}$$

in terms of the Higgs doublet Φ, the left-handed quark and lepton $SU(2)$ doublets Q_L and L_L, and the right-handed up, down, and lepton singlets u_R, d_R, and e_R. We have suppressed generation indices and consider the 3×3 matrices of Wilson coefficients $\tilde{c}_{U,D,L}$ to be diagonal and real (such that the operators are purely CP violating). The extension to include flavor-changing operators can be made straightforwardly. Again, we assume the dimension-six Yukawa couplings to be proportional to the SM Yukawa couplings $y_f/\sqrt{2} = m_f/v_0$ ($v_0 \simeq 246$ GeV is the zero-temperature vev) as is the

case in many BSM scenarios and suggested by minimal flavor violation

$$\tilde{Y}_U = \mathrm{diag}(y_u\tilde{c}_u,\, y_c\tilde{c}_c,\, y_t\tilde{c}_t)\,,\quad \tilde{Y}_D = \mathrm{diag}(y_d\tilde{c}_d,\, y_s\tilde{c}_s,\, y_b\tilde{c}_b)\,,\quad \tilde{Y}_L = \mathrm{diag}(y_e\tilde{c}_e,\, y_\mu\tilde{c}_\mu,\, y_\tau\tilde{c}_\tau)\,. \tag{7.2}$$

Finally, we write

$$\tilde{c}_f = \frac{s_f}{\Lambda_f^2}\,, \tag{7.3}$$

where $s_f = \pm 1$ is chosen to obtain a net number of baryons (rather than antibaryons) and Λ_f is the associated scale of new physics where the EFT breaks down. We stress that these operators are still just a subset of dimension-six SM-EFT CPV operators that can be constructed. The above operators are particularly efficient in generating a baryon asymmetry as they give rise to an effective CPV mass term during the phase transition, as we have seen in section 5.3. In addition to SM-EFT operators, in principle there can be CPV operators that include the unspecified light scalar degrees of freedom, which can only be included if we consider a specific UV completion of the scalar sector. We focus instead on the operators in eq. (7.1) as these can readily be constrained by EDM experiments.

The transport equations and the expressions for the relaxation rates and CPV source term are given in section 5.3. For later convenience, we define the function $J_f(T)$ through:

$$S_f = \frac{v_w N_c}{2\pi^2}\mathrm{Im}\left[g_f' g_f^*\right] J_f(T)\,, \tag{7.4}$$

where $J_f(T)$ is the integral in eq. (5.27) and the function g_f which was defined in eq. (5.19) should be computed for the appropriate fermion.

7.2.3 Experimental constraints on CP-violating dimension-six operators

The computation of the EDM constraint on the various CPV scales is analogous to the computation in section 6.2.1. As we will argue, for EWBG purposes the only relevant interactions are those involving the top, bottom, and tau and we mainly discuss these. Couplings to lighter fermions are too weak to create sufficient baryon asymmetry.

The contributions to the two-loop Barr-Zee diagrams of the top, bottom and tau fermions are given by [288, 289, 300]

$$\frac{d_e}{e} = -\frac{8\alpha_{em}}{(4\pi)^3} m_e \left[N_c Q_t^2\, g(x_t)\,\frac{s_t}{\Lambda_t^2} + N_c Q_b^2\, g(x_b)\,\frac{s_b}{\Lambda_b^2} + Q_\tau^2\, g(x_\tau)\,\frac{s_\tau}{\Lambda_\tau^2}\right]\,, \tag{7.5}$$

where Q_f denotes the fermion charge in units of e, $x_f = m_f^2/m_h^2$, and $g(x_f)$ the two-loop function

$$g(x_f) = \frac{x_f}{2}\int_0^1 dx\,\frac{1}{x(1-x)-x_f}\log\left(\frac{x(1-x)}{x_f}\right). \tag{7.6}$$

Numerically we have $g(x_t) \simeq 1.4$, $g(x_b) \simeq 2.7\cdot 10^{-2}$, $g(x_\tau) \simeq 7.7\cdot 10^{-3}$, and for lighter fermions the function roughly scales as $g(x_f) \sim x_f \log x_f$.

The recent constraint on the electron EDM from the ACME experiment $d_e \leq 1.1\times 10^{-29}\,e\,\text{cm}$ at 90% c.l. [297] puts a strong constraint on the CPV dimension-six top interaction $\Lambda_t \geq 7.1$ TeV, as we already saw in chapter 6. For the bottom and charm we find $\Lambda_b \geq 0.49$ TeV and $\Lambda_c \geq 0.41$ TeV and for the tau $\Lambda_\tau \geq 0.16$ TeV. For the lighter fermions no meaningful constraint can be set as the limit on Λ_f is lower than the electroweak scale. The tau coupling can in principle also be constrained by the limit on the tau EDM. However, while the contribution to the tau EDM from CPV tau-couplings is about a factor $\mathcal{O}(10^6)$ larger than the contribution to the eEDM, the experimental limit on the tau EDM is roughly a factor $\mathcal{O}(10^{11})$ weaker [336] and no significant constraints are obtained. The story is similar for the CPV μ-Higgs coupling and no significant constraint can be set. A CPV e-Higgs coupling, however, would lead to a large eEDM and we get a limit $\Lambda_e \geq 5.7$ TeV [337].

Additional constraints can be set by using experimental limits on hadronic EDMs. In this case, the analysis is more complicated and requires apart from several additional one- and two-loop diagrams also renormalization-group evolution factors and hadronic and nuclear matrix elements. A detailed study can be found in Refs. [289, 338]. With conservative values of matrix elements linking CP-odd quark-gluon operators to the neutron and Hg EDMs, we obtain $\Lambda_t \geq 0.7$ TeV, which is significantly weaker than the eEDM constraints, while no significant constraints can be set on Λ_b. For completeness we also give the EDM constraints for lighter quarks. Using conservative values for hadronic matrix elements there is no significant constraint for Λ_s and Λ_c, while $\Lambda_d \geq 1$ TeV and $\Lambda_u \geq 0.5$ TeV [289, 338]. Despite these weaker limits, we will see that EWBG is not efficient for CPV couplings involving light quarks.

The CPV fermion-Higgs couplings can also be probed at the LHC. At present, measurements of genuine CP-odd observables are not precise enough to set meaningful constraints. However, the CPV couplings modify also CP-even observables via contributions proportional to $\tilde{c}_f^2 \sim 1/\Lambda_f^4$. For example, the CPV tau-Higgs coupling modifies the $h\to\tau\tau$ branching ratio signal strength

$$\mu_{h\to\tau\tau} = \frac{\Gamma_{h\to\tau\tau}}{\Gamma^{SM}_{h\to\tau\tau}}\frac{\Gamma_h^{SM}}{\Gamma_h} = 1 + \frac{v^4}{\Lambda_\tau^4}\left(\frac{1}{1-4x_\tau}\right)\left(1 - \frac{m_H m_\tau^2}{8\pi v^2}\frac{(1-x_\tau)^{3/2}}{\Gamma_h^{\text{SM}}}\right), \tag{7.7}$$

where Γ_h denotes the total Higgs width in the presence of the CPV operators and $\Gamma_h^{\rm SM} \simeq 4.1$ MeV the predicted SM Higgs width. $\mu_{h\to\tau\tau}$ has been measured by ATLAS, $\mu_{h\to\tau\tau} = 1.09^{+0.18+0.27+0.16}_{-0.17-0.22.-0.11}$ [339]. Adding the uncertainties in quadrature gives the constraint $\Lambda_\tau \gtrsim 0.3$ TeV. Such limits are thus not very stringent. Similar analyses can be performed for other fermions, but in all cases the bounds on Λ_f are well below 1 TeV [289].

7.2.4 Transport equations

We use the set of transport equations given in eq. (5.32). If the new degrees of freedom that provide the first-order phase transition also couple to SM fermions additional interaction rates can appear in the transport equations. We model one such possible term by adding a $\Gamma_{\rm QL}$ that corresponds to a new top-tau interaction. This coupling will be motivated in section 7.2.5. It modifies the equations for q, t, l and τ, which we list here.

$$\begin{aligned}
\partial_\mu q^\mu &= +\Gamma_M^{(t)}\mu_M^{(t)} + \Gamma_M^{(b)}\mu_M^{(b)} + \Gamma_Y^{(t)}\mu_Y^{(t)} + \Gamma_Y^{(b)}\mu_Y^{(b)} - 2\,\Gamma_{\rm ss}\,\mu_{\rm ss} + \Gamma_{\rm QL}\,\mu_{\rm QL} - S_t - S_b\,,\\
\partial_\mu t^\mu &= -\Gamma_M^{(t)}\mu_M^{(t)} - \Gamma_Y^{(t)}\mu_Y^{(t)} + \Gamma_{\rm ss}\,\mu_{\rm ss} - \Gamma_{\rm QL}\,\mu_{\rm QL} + S_t\,,\\
\partial_\mu l^\mu &= +\Gamma_M^{(\tau)}\mu_M^{(\tau)} + \Gamma_Y^{(\tau)}\mu_Y^{(\tau)} - \Gamma_{\rm QL}\,\mu_{\rm QL} - S_\tau\,,\\
\partial_\mu \tau^\mu &= -\Gamma_M^{(\tau)}\mu_M^{(\tau)} - \Gamma_Y^{(\tau)}\mu_Y^{(\tau)} + \Gamma_{\rm QL}\,\mu_{\rm QL} + S_\tau\,.
\end{aligned} \tag{7.8}$$

The other transport equations in eq. (5.32) are unaffected. The chemical potential corresponding to the new interaction is

$$\mu_{\rm QL} = \left(\frac{l}{k_l} - \frac{\tau}{k_\tau} - \frac{q}{k_q} + \frac{t}{k_t}\right)\,. \tag{7.9}$$

In principle, we should also add a transport equation for the new light degrees of freedom added to the scalar sector. Generically, these new degrees of freedom equilibrate with the SM Higgs as significant interactions are required for a first-order phase transition, and the scalar degrees of freedom can be added to h which now denotes a combined number density.

The complete expressions for the interaction rates, source terms, masses, and other constants entering the equations can be found in section 5.3 and Appendix A. In this chapter we solve the transport equations numerically, with the boundary condition that the number densities vanish far away from the bubble wall. Details can be found in Appendix C of Ref. [4]. As an extra check we also solve the equations using the semi-analytical method that we used in chapter 6. Both approximations are reasonable, and for generic input parameters we find that the numerical and semi-analytical results

only differ by $\mathcal{O}(10\%)$. Unless otherwise stated, the results presented in the upcoming sections are those of the numerical calculation. We obtain the value of the baryon asymmetry from eq. (5.38).

7.2.5 Efficiency of quark/lepton source

A priori, one would expect the top source to give the largest baryon asymmetry. Since the CPV source term of eq. (7.4) is proportional to the Yukawa coupling squared, it is maximal for the top quark. Even if we had not assumed the dimension-six couplings to be proportional to y_f, the source would have a linear dependence on the Yukawa coupling. A first reason why the top-source scenario might nevertheless not be the most efficient mechanism to generate the BAU is also immediately apparent from eq. (7.4). The CPV source is suppressed by the square of the scale Λ_f. In section 7.2.3 we showed that the experimental bounds on Λ_f are rather strong for the top quark: $\Lambda_t \gtrsim 7.1\,\text{TeV}$. For the bottom quark and the tau lepton the bounds are much less severe: $\Lambda_b \gtrsim 0.5\,\text{TeV}$ and $\Lambda_\tau \gtrsim 0.3\,\text{TeV}$ respectively.

A second reason why leptons could be more efficient than quarks in generating the BAU is their larger diffusion coefficient. Since leptons only interact via the electroweak force they can diffuse further into the symmetric phase than the strongly interacting quarks [323]. This enhances the baryon asymmetry, as the electroweak sphalerons have more time to convert the lepton asymmetry into a baryon asymmetry before the bubble wall passes.

Finally, washout effects are also maximal for top quarks. The interactions mediated by the CP conserving part of the mass matrix relax the chiral asymmetry; the relaxation rate for this process is proportional to $\Gamma_M^{(f)} \propto |g_f|^2 = y_f^2\varphi_b^2 + \mathcal{O}(\Lambda_f^{-4})$, and thus largest for the top quark. The rate for Yukawa-type interactions (with radiation of an additional gluon or weak boson) is likewise maximized for the top quark $\Gamma_Y^{(f)} \propto y_f^2$.

More importantly, the strong sphaleron transitions are approximately in equilibrium in the symmetric phase except for regions close to the bubble wall [311, 314, 324] — we will estimate the size of this region in section 7.4.1 — and they very effectively wash out the chiral asymmetry in the quark sector, but leave leptons untouched. Indeed, if the strong sphaleron interactions are in thermal equilibrium the corresponding chemical potential eq. (5.33) vanishes $\mu^{ss} \simeq 0$. Neglecting the Yukawa interactions of the first- and second-generation quarks, and using baryon number conservation gives the relation

$$-4ua_1 + qa_2 + ba_3 \simeq 0\,, \tag{7.10}$$

where

$$a_1 = \frac{1}{2}\left(\frac{4}{k_{q_1}} + \frac{1}{k_u} + \frac{1}{k_d}\right), \quad a_2 = \left(\frac{2}{k_q} + \frac{1}{k_t}\right), \quad a_3 = \left(\frac{1}{k_t} - \frac{1}{k_b}\right). \tag{7.11}$$

The chiral asymmetry in quarks becomes

$$n_L^{(q)} \equiv \sum_{i=1}^{3} q_i = q - 4u = q\left(1 - \frac{a_2}{a_1}\right) - b\left(\frac{a_3}{a_1}\right), \tag{7.12}$$

where in the second and third steps we used eq. (5.31) and eq. (7.10), respectively. At zero temperature $(a_1, a_2, a_3) \propto (1, 1, 0)$ and the chiral asymmetry in quarks vanishes. At finite temperature there are corrections. For our benchmark point we find $n_L^{(q)} \simeq -0.01q - 0.01b$, and thus the chiral asymmetry in quarks is suppressed by roughly two orders of magnitude with respect to the individual quark densities. Note that we already studied this effect in section 6.5, but there we did not include the bottom quarks.

The above reasons ensure that the tau-source scenario is more effective at producing the baryon asymmetry than the top-source scenario. That is, despite the Yukawa suppression of the tau source we will obtain similar values of the total baryon asymmetries for $\Lambda_t \simeq \Lambda_\tau$.

The top Yukawa and especially the strong sphaleron interactions are very effective in washing out the chiral asymmetry in quarks. Hence, if, in the case of CP violation in the quark sector, part of the chiral asymmetry can be transferred to the leptons, which will escape the washout, the baryon asymmetry is increased. Leptons produced via the relatively small tau Yukawa interactions give the dominant contribution to the baryon asymmetry in the top-source scenario leading to a larger asymmetry up to an order of magnitude (see figure 7.3). The authors of Refs. [273, 315, 323] already pointed out that the contribution of tau leptons can be significant in the context of a two Higgs doublet model and the MSSM where the value of y_τ can be boosted by a large $\tan\beta$, but we stress that this Yukawa enhancement is not required for leptons to be very relevant. This relevance can be even enhanced in models with additional chiral-symmetry-breaking lepton-quark interactions, for instance via the exchange of new scalars. We discuss this in the next section.

7.2.6 Additional chiral-symmetry-breaking quark-lepton interactions

The importance of the leptons in the top-source case becomes even more pronounced in models with additional chiral-symmetry-breaking quark-lepton interactions. In our set-up we have added a dimension-six tau-top interaction to study this effect, but the qualitative results are insensitive to

the exact implementation. The dimension-six operator is given by

$$\mathcal{L}_{\mathrm{QL}} = \frac{1}{\Lambda_{\mathrm{QL}}^2}\bar{\tau}_L\tau_R\bar{t}_R t_L + \mathrm{h.c.}\,. \tag{7.13}$$

Using the methods of Ref. [325] we have calculated the rate associated to this interaction and obtain $\Gamma_{\mathrm{QL}} = \kappa_{\mathrm{QL}} T^5/\Lambda_{\mathrm{QL}}^4$ with κ_{QL} a factor of $\mathcal{O}(1)$. This interaction becomes important if it exceeds the SM tau Yukawa rate, which, for our benchmark point, is the case for $\Lambda_{\mathrm{QL}} \lesssim 3\,\mathrm{TeV}$.

For definiteness, we focus here on a new top-tau coupling but stress that a coupling to the muon or electron has a similar effect. If the CPV source is located in the quark sector, the baryon asymmetry can also be boosted by including a new coupling of the top to one of the lighter quarks (e.g. a top-charm coupling). In such a scenario the washout by strong sphalerons becomes less effective. Indeed, eq. (7.12) above was derived under the assumption that the light quarks are only produced via strong sphalerons and that their Yukawa interactions are negligible, such that eq. (5.31) holds. If, say, the new top-charm interaction is stronger than the strong sphaleron interactions, this is no longer the case, and the washout by strong sphalerons no longer implies a washout of the chiral asymmetry.

On the other hand, if the CPV source is located in the lepton sector, presence of the new top-tau interaction reduces the value of the baryon asymmetry. Part of the chiral asymmetry produced in the lepton sector now gets transported to the quark sector, where it gets washed out by strong sphalerons and top Yukawa interactions.

We describe the top-tau transfer here with an effective interaction, but larger interaction rates are possible if the coupling is via exchange of a light degree of freedom, for example the new scalar particle added to get a first-order phase transition [326, 327]. In such cases the scattering can be resonantly enhanced. To properly describe this requires the inclusion of the transport equation for the light particle with the corresponding interaction rates derived from renormalizable interactions. We expect that our effective interaction gives qualitatively similar results, even in the regime where Λ_{QL} is fairly small, and we therefore treat Λ_{QL} as a phenomenological parameter. We will show in section 7.5 that such interactions, even of modest strength, can drastically increase or reduce the baryon asymmetry depending on the nature of the CPV source.

7.3 Baryogenesis with a tau-lepton source

We start with a discussion of baryogenesis from a CPV tau source, and assume there is no new lepton-quark coupling (that is, we set $\Lambda_{\rm QL} \to \infty$). The value of the tau Yukawa coupling at the electroweak scale is small, $y_\tau \simeq 0.01$, with respect to the top Yukawa coupling, $y_t \simeq 1$. For reasons discussed in section 7.2.5, the tau could nevertheless be an interesting source of the baryon asymmetry.

In the present scenario, the lepton sector essentially decouples from the quark sector and the baryon asymmetry can be computed analytically to good accuracy. We start with discussing the analytical approximation and later compare it to the full numerical solution that *does* include effects of the quark sector. The analytical solution clarifies the dependence of the baryon asymmetry on parameters associated to the bubble wall and the leptonic Yukawa couplings. This relatively simple set-up provides insight into more complicated scenarios where analytical solutions are not possible.

7.3.1 Analytical approximation

The transport equations in eq. (5.32) contain separate equations for the third-generation left-handed doublet, l^μ, and the right-handed singlet, τ. Because the left- and right-handed tau leptons diffuse at different rates: $D_l = 100/T$ and $D_\tau = 380/T$ [273], in principle we have to treat these number densities separately. However, to a reasonable approximation we can ignore this difference and set $D_l = D_\tau = 100/T$, which implies $l = -\tau$. The lepton transport equation simply becomes

$$-D_l l'' + v_w l' + \bar{\Gamma} l - \Gamma_Y^{(l)} \frac{h}{k_h} = -S_\tau \,, \qquad \text{with} \qquad \bar{\Gamma} = \left(\Gamma_M^{(l)} + \Gamma_Y^{(l)}\right)\left(\frac{1}{k_\tau} + \frac{1}{k_l}\right). \tag{7.14}$$

CPV resides in the lepton sector and any non-zero density of Higgs particles can only be generated via interactions with leptons. Since the lepton Yukawa rate is relatively slow the Higgs density remains small and we can approximate $h \simeq 0$. In this limit, the leptons decouple completely and to find the chiral asymmetry we only have to solve eq. (7.14). This can be done using the semi-analytical solution that we used in chapter 6 (see section 6.5), which gives

$$l = -\frac{2\bar{S}}{(\sqrt{4D_l\bar{\Gamma}_B + v_w^2} + \sqrt{4D_l\bar{\Gamma}_S + v_w^2})} \mathrm{e}^{z/L_S} \,, \quad \text{for } \; z < 0 \,, \tag{7.15}$$

with $\bar{\Gamma}_{\{S,B\}}$ the rescaled interaction rates (7.14) in the symmetric and broken phase respectively, and

$$\begin{aligned} L_i &= \frac{2D_l}{\left(v_w + \sqrt{4D_l\bar{\Gamma}_i + v_w^2}\right)}\,, \\ \bar{S} &= \int_0^\infty \mathrm{e}^{-y/L_B} S_\tau(y)\mathrm{d}y = \frac{15 s_\tau}{128\pi^2}\frac{y_\tau^2}{\Lambda_\tau^2} v_w v_N^4 J_\tau(T)\left[1 - \frac{4(7+6\ln 2)}{45}\frac{L_w}{L_B} + \mathcal{O}\left(\frac{L_w^2}{L_B^2}\right)\right], \end{aligned} \tag{7.16}$$

and $i = \{S, B\}$. To get the second expression for $\bar{S}$, we used eqs. (5.15) and (7.4), and expanded in L_w/L_B. For a tau source, the leading order term dominates by far and we can set $L_w/L_B \simeq 0$.

Integrating the chiral asymmetry, $n_L = l$, as in eq. (5.38) gives the baryon asymmetry

$$Y_B = \frac{3\Gamma_{\rm ws}}{2v_w s}\frac{2\bar{S}}{(\sqrt{4D_l\bar{\Gamma}_B + v_w^2} + \sqrt{4D_l\bar{\Gamma}_S + v_w^2})}\frac{L_{\rm ws}L_S}{L_S + \frac{1}{2}L_{\rm ws}\left(1 + \sqrt{1 + \frac{4D_q}{L_{\rm ws}v_w}}\right)}\,, \tag{7.17}$$

with $L_{\rm ws} = v_w/(\mathcal{R}\Gamma_{\rm ws})$. Noting that $J_\tau < 0$, we have to pick $s_\tau = -1$ for the sign of the CPV coupling, to get the right sign for the baryon asymmetry. The last factor in eq. (7.17) arises from

$$I_Y \equiv \int \mathrm{d}z\, \mathrm{e}^{z\left(L_S^{-1} - \alpha_-\right)} = \frac{L_{\rm ws}L_S}{L_S + \frac{1}{2}L_{\rm ws}\left(1 + \sqrt{1 + \frac{4D_q}{L_{\rm ws}v_w}}\right)}\,, \tag{7.18}$$

with α_- as defined in eq. (5.38).

7.3.2 Comparison of approximations

We have calculated the total baryon asymmetry using different approximations:

1. The analytical solution in eq. (7.17) of the purely leptonic transport equation, eq. (7.14), where the Higgs and quark sectors are neglected. We call this solution $A(l)$.
2. A numerical solution of eq. (7.14) called $N(l)$.
3. A numerical solution that includes the Higgs and third-generation quarks called $N(l, h, q, t)$.
4. Finally, we investigate the different diffusion constants of left- and right-handed leptons. That is, we allow $D_l \neq D_\tau$ in $N(l, \tau)$. For numerical reasons we study this effect in the limit of a decoupled quark sector.

The entries in brackets in $A(...)$ and $N(...)$ denote the number densities for which we solve the transport equation explicitly in the respective approximation. In scenarios where the quark sector is

Approximation	A(l)	N(l)	N(l, h, q, t)	N(l, τ)
Y_B	6.8×10^{-11}	7.3×10^{-11}	7.3×10^{-11}	8.2×10^{-11}

TABLE 7.1: Baryon asymmetry Y_B for a tau CPV source obtained using various approximations as detailed in the main text. We used the benchmark values for the bubble-wall profile given in section 7.2.1 and $\Lambda_\tau = 1$ TeV.

considered, we apply local baryon conservation, eq. (5.37), and the relation in eq. (5.31) to account for the number densities of the bottom and lighter quarks.

The resulting baryon asymmetries in the various approximations for our benchmark point with $\Lambda_\tau = 1\,\text{TeV}$ and bubble-wall velocity $v_w = 0.05$ are given in table 7.1. Comparing N(l, τ) to N(l) shows that local lepton conservation is a reasonable approximation. More importantly, the analytical solution differs only $\sim 10\%$ from the numerical solutions with and without inclusion of the Higgs and quark sectors, that is from N(l, h, q, t) and N(l) respectively. The tau Yukawa coupling is sufficiently small that decoupling the Higgs and quark sectors is an excellent approximation.

In the left panel of figure 7.1 the various approximations are compared while varying the value of the tau Yukawa coupling. The decoupling approximation works well up to $y_\tau \lesssim 0.2$ while for larger values significant Higgs and quark densities are generated. The right panel of figure 7.1 shows that the analytical approximation holds over a large range of bubble-wall velocities, such that the conclusions are not restricted to just our benchmark values.

7.3.3 Parameter dependence

Having found that the analytical solution provides an excellent approximation, we can use it to understand how the baryon asymmetry depends on various parameters, such as the Yukawa coupling and the parameters associated to the bubble wall. It is useful to rewrite the solution for Y_B in eq. (7.17) in terms of various length scales

$$Y_B = \frac{3}{s\mathcal{R}} \frac{\bar{S}}{v_w L_{\text{ws}}} \frac{1}{\sqrt{1 + 4\frac{L_{\text{diff}}}{L^S_{\text{int}}}} + \sqrt{1 + 4\frac{L_{\text{diff}}}{L^B_{\text{int}}}}} \frac{L_{\text{ws}} L_S}{L_S + \frac{1}{2} L_{\text{ws}} \left(1 + \sqrt{1 + 4\frac{L^q_{\text{diff}}}{L_{\text{ws}}}}\right)}, \tag{7.19}$$

which are defined in table 7.2. L_S and L_B determine how far the asymmetry migrates into, respectively, the symmetric and broken phase. On larger length scales the asymmetry is exponentially suppressed by the $e^{-|z|/L_i}$-factor in eqs. (7.15) and (7.16). $L_{\text{diff}} = D_l/v_w$ is the diffusion length, which determines how far the asymmetry can diffuse into the symmetric phase before it is overtaken by the expanding bubble.

Length scale	Description	Benchmark value
$L_S = \frac{2L_{\rm diff}}{1+\sqrt{1+4L_{\rm diff}/L_{\rm int}^S}}$	migration length in symmetric phase	21.3
$L_B = \frac{2L_{\rm diff}}{1+\sqrt{1+4L_{\rm diff}/L_{\rm int}^B}}$	migration length in broken phase	9.8
$L_{\rm int}^S = v_w/\bar{\Gamma}_S$	interaction length in symmetric phase	313.3
$L_{\rm int}^B = v_w/\bar{\Gamma}_B$	interaction length in broken phase	7.0
$L_{\rm diff} = D_l/v_w$	lepton diffusion length	22.7
$L_{\rm diff}^q = D_q/v_w$	quark diffusion length	1.4
$L_{\rm ws} = v_w/(\mathcal{R}\Gamma_{\rm ws})$	weak sphaleron length	28.5
L_w	bubble-wall width	0.1

TABLE 7.2: Length scales (in units of GeV^{-1}) for a tau CPV source and their values for the benchmark values for the bubble-wall profile given in section 7.2.1 and $\Lambda_\tau = 1$ TeV.

The interaction lengths in the symmetric and broken phase are denoted by $L_{\rm int}^i = v_w/\bar{\Gamma}_i$ with $i = S, B$, respectively. If interactions are slow, $L_{\rm diff} \ll L_{\rm int}^i$, they can be neglected, and the migration scale is determined by diffusion $L_i \simeq L_{\rm diff}$. In the opposite limit of fast interactions, the symmetry is washed out over scales larger than $L_i \simeq \sqrt{L_{\rm diff} L_{\rm int}^i} = \sqrt{D_l/\bar{\Gamma}_i}$. In the broken phase, L_B has to be compared with the spatial extend of the source, which is set by the bubble-wall width L_w. For $L_w \ll L_B$ the source is not diluted by diffusion nor interactions and we can approximate $\bar{S}$ by the first term in eq. (7.16).

The conversion of the chiral number into a net baryon number through eq. (5.38) introduces additional length scales: the baryon/quark diffusion length scale $L_{\rm diff}^q = D_q/v_w$, and the scale on which the weak sphalerons act $L_{\rm ws} = v_w/(\mathcal{R}\Gamma_{\rm ws})$. In the limit $L_S \ll L_{\rm ws}$ the migration length, i.e., how far the chiral asymmetry migrates into the symmetric phase, determines the extend of the region in front of the bubble wall that contributes to the baryon asymmetry and the integral (7.18) becomes $I_Y \simeq L_S$. In the opposite limit, $L_{\rm ws} \ll L_S$, it seems necessary to include the weak sphaleron interactions directly in the transport equations, as there is no hierarchy between the sphaleron and Yukawa interactions, invalidating the two step procedure. However, although both processes may be important for the final asymmetry (depending on the bubble-wall velocity) they are still very far from equilibrium, and backreaction effects are small. It was checked numerically that the two-step procedure used to derive eq. (7.17) is a good approximation to the full coupled set of equations, see Appendix B of Ref. [4] for more details. We then find that in this regime the integral is cut off by $L_{\rm ws}$, the scale on which the weak sphalerons act, and $I_Y \simeq L_{\rm ws}(1+\sqrt{r})^{-1}$ in the parameter regime of interest, with

$$r = \frac{L_{\rm ws} L_{\rm diff}^q}{L_S^2} \overset{v_w \to 0}{=} \frac{D_q}{D_l} \frac{\bar{\Gamma}_S}{\mathcal{R}\Gamma_{\rm ws}}\,, \tag{7.20}$$

where the right-hand expression is valid in the small-velocity limit where r is maximal. For the tau Yukawa interactions $r \ll 1$ and we can neglect the baryon diffusion effects, and the approximation made in eq. (5.39) holds. This is no longer the case for the top- and bottom-source scenarios discussed in section 7.4, as can be anticipated from the above estimate. Replacing the tau Yukawa interaction with the top Yukawa or strong sphaleron interaction, and setting $D_l \to D_q$ gives $r \gg 1$.

The various length scales are listed in table 7.2, along with their value for the benchmark point. The length scales depend on bubble-wall parameters such as v_N and v_w that we can vary depending on the electroweak phase transition, and on SM parameters such as the tau Yukawa coupling, y_τ. We also consider variations in y_τ to see what would happen for source terms involving lighter SM fermions and to get some (limited) insight about what happens for heavier quarks, as further discussed in the next section. For all parameter choices, we have $L^B_{\rm int} \ll L^S_{\rm int}$ as $\Gamma^{(l)}_M$ greatly exceeds the Yukawa interaction rate in both the symmetric and broken phase. The solution for the baryon asymmetry can then be divided into three[1] different regions, depending on the chosen parameters and the resulting sizes of the relevant length scales:

a $L_{\rm diff} < L^B_{\rm int}, L^S_{\rm int}, L_{\rm ws}$ which corresponds to small Yukawa couplings and a large bubble-wall velocity. Interactions are slow and can be neglected, and the chiral asymmetry diffuses without washout $L_i \simeq L_{\rm diff}$. Since the diffusion length is much larger than the source width $L_{\rm diff} \gg L_w$ there is no dilution of the source and the expansion in eq. (7.16) is valid. In this regime, the baryon asymmetry becomes

$$Y_B \simeq \frac{3}{2s\mathcal{R}} \frac{\bar{S}}{v_w} \frac{L_{\rm diff}}{L_{\rm ws}} \propto \frac{y_\tau^2}{v_w^2} \frac{1}{\Lambda_\tau^2} \,. \tag{7.21}$$

The asymmetry decreases for large bubble-wall velocity, which can be understood as the faster the bubble moves, the less time there is for the chiral asymmetry to diffuse into the symmetric phase and to be converted into a baryon asymmetry. The asymmetry decreases quadratically with a smaller Yukawa coupling, which originates from the scaling of the source. In practice, the tau Yukawa coupling is slightly too large for the above scaling to hold for the benchmark velocity $v_w \simeq 0.05$.

b $L^B_{\rm int} < L_{\rm diff} < L^S_{\rm int}, L_{\rm ws}$. Interactions are now important in the broken phase and $L_B \simeq \sqrt{L^B_{\rm int} L_{\rm diff}}$. The dilution of the source in $\bar{S}$ is still a negligible effect, as $L_B \simeq L_w$ only holds for $\mathcal{O}(1)$ Yukawa couplings. The interactions in the broken phase, however, change the baryon

[1] In principle there exists a fourth region $L^S_{\rm int} \ll L_{\rm diff}$ and $L_S = \sqrt{L^S_{\rm int} L_{\rm diff}} \ll L_{\rm ws}$. This requires $\mathcal{O}(1)$ Yukawa couplings, for which our analytical approximation eq. (7.15) breaks down. As this is not the physical region of interest, we do not discuss this possibility further.

asymmetry into

$$Y_B \simeq \frac{3}{2s\mathcal{R}}\frac{\bar{S}}{v_w}\frac{\sqrt{L_{\rm diff}L^B_{\rm int}}}{L_{\rm ws}} \propto \frac{y_\tau}{v_w}\frac{1}{\Lambda_\tau^2}\,. \tag{7.22}$$

Y_B thus scales linearly with the Yukawa coupling and inversely with the bubble velocity. Here we see for the first time a violation of the naive y_f^2 scaling of the asymmetry.

c $L^B_{\rm int} < L_{\rm ws} < L_{\rm diff}, L^S_{\rm int}$ which corresponds to small velocities (and $y_\tau \lesssim 0.2$ such that the analytical approximation is valid). The baryon asymmetry

$$Y_B \simeq \frac{3}{2s\mathcal{R}}\frac{\bar{S}}{v_w}\sqrt{\frac{L^B_{\rm int}}{L_{\rm diff}}} \propto \frac{y_\tau v_w}{\Lambda_\tau^2}\,, \tag{7.23}$$

now scales linearly with both y_τ and v_w. The asymmetry decreases for small velocity, as in this limit the evolution approaches thermal equilibrium. We neglect the $L^S_{\rm int}$ dependence in the denominator in eq. (7.17) as it is subdominant to the $L^B_{\rm int}$ term.

Comparing eqs. (7.22) and (7.23) it follows that the asymmetry is maximized as a function of the velocity at the boundary of the two regimes, that is, for $L_{\rm ws} \sim L_{\rm diff}$. For the SM tau Yukawa coupling, region **a** corresponds to $v_w \gtrsim 0.1$, region **b** to $0.04 \lesssim v_w \lesssim 0.1$, and region **c** to $v_w \lesssim 0.04$.

The scaling of the asymmetry with bubble-wall velocity and Yukawa coupling are illustrated in figure 7.1. The left panel shows Y_B as a function of the Yukawa coupling y_τ. The vertical thick line gives the boundary between region **a** and **b**; region **c** does not occur for our benchmark velocity. In region **a**, on the left of the vertical thick line, the baryon asymmetry scales quadratically with the small Yukawa coupling, while in region **b**, on the right, the scaling is linear. The SM Yukawa value $y_\tau = 0.01$ falls in region **b**, and the baryon asymmetry for this value is indicated by a star (and corresponds to our benchmark number in table 7.1). The most relevant observation is that for $y_\tau \geq 0.005$, Y_B only grows linear with y_τ instead of the naively expected quadratic scaling. This confirms that CPV sources for fermions lighter than top quarks are less disadvantageous than might be expected.

The right panel shows Y_B as a function of the bubble-wall velocity v_w. Now the black lines divide, from right to left, regions **a**, **b**, and **c** that scale respectively as v_w^{-2}, v_w^{-1} and v_w. The boundary between **b** an **c** corresponds to the velocities for which $L_{\rm ws} \sim L_{\rm diff}$, approximately where the baryon asymmetry is maximized. Our benchmark point lies in scenario **b**, very close to the optimum value.

We end this section with a short discussion of how the baryon asymmetry depends on the dynamics of the first-order phase transition that we have parameterized by the bubble-wall profile eq. (5.15).

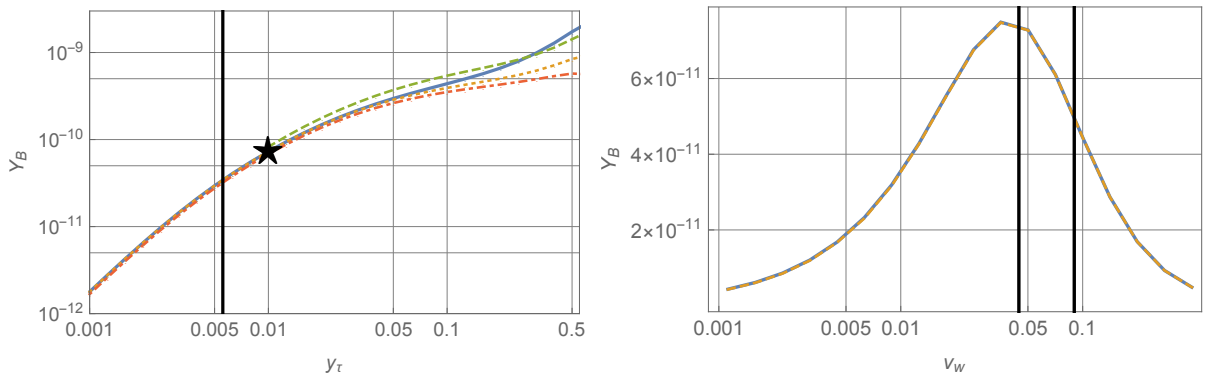

FIGURE 7.1: Left: Y_B as a function of the Yukawa coupling y_τ for the same four approximations as in Table 7.1 (solid blue: N(l,h,q,t), dotted orange: N(l), dashed green N(l,τ), dotdashed red: A(l)). The region left (right) of the vertical black line corresponds to region **a** (**b**). The star denotes the SM value of y_τ.
Right: Y_B as a function of the bubble-wall velocity v_w (solid blue: $N(l,h,q,t)$, dashed orange: N(l)). The left, middle and right regions corresponds to regions **c**, **b**, and **a**, respectively.

The bubble-wall width only enters the equations via the source. In the limit that $L_w/L_B \ll 1$, as appropriate for a tau source, the dependence on this parameter cancels. A larger bubble wall width gives a wider source but with a smaller amplitude, such that the total integrated source $\bar{S}$ remains the same.

The source scales as $\bar{S} \propto v_N^4$ with v_N the Higgs vev during nucleation; this power comes about because of the structure of our dimension-six CPV operator which involves three Higgs fields[2]. The relaxation rate $\Gamma_M^{(f)} \propto v_N^2$ depends on the vev as well. It thus follows that in region **a**, the baryon asymmetry scales as $Y_B \propto v_N^4$ and in region **b** as $Y_B \propto v_N^3$. For the SM tau Yukawa coupling we are in region **b**, but the velocity dependence of L_B cannot be fully neglected and numerically we find a scaling $Y_B \propto v_N^{3.2}$. Although the dependence on the vev is strong, we do not expect v_N to vary too much between different BSM models.

The dependence on the nucleation temperature T_N is harder to estimate, as many parameters, such as the thermal masses and thermal width, depend on the temperature. All interaction rates scale as $\Gamma_i \propto T$, except for $\Gamma_M \propto 1/T$; further $D_i \propto 1/T$ and $S \propto T$. With this scaling we find that $Y_B \propto 1/T_N^2$ in regime **a** and $Y_B \propto 1/T_N$ in regime **b**. We note that as T_N increases the relative importance of L_{int}^B decreases, and we move from regime **b** to **a**.

[2]In two-Higgs doublet models CPV can originate from dim-4 operators, in which case the corresponding source would only scale quadratically with the vev.

7.3.4 Producing the universal baryon asymmetry with a tau source

Can CP violation in the lepton sector produce the observed baryon asymmetry? The asymmetry for the benchmark point in table 7.1 is fairly close to the observed value in eq. (5.1). The scale $\Lambda_\tau \sim 1\,\text{TeV}$ is fairly low, but not inconsistent with EDM and collider experiments. It could be even lowered somewhat to further increase Y_B but the EFT description becomes problematic for such low scales. As shown in the right panel of figure 7.1 the benchmark $v_w = 0.05$ is already close to optimal, and there is little room for improvement. Definite statements about the viability of the scenario are not easy to make, as the performed calculations still suffer from uncertainties, such as those related to the description of the phase transition, that are hard to quantify. We refer to e.g. Ref. [226] for a more general discussion of outstanding problems in calculations of EWBG. Nevertheless, our analysis indicates that CPV sources in the tau sector are viable despite the small Yukawa coupling and not yet significantly constrained by EDM experiments.

Our study of the dependence of Y_B on the value of y_τ can be directly used to study the cases of CP-violating electron and muon source terms. In such cases, the transport equations are identical after replacing the third-generation lepton number densities with the first- or second-generation densities and rescaling the $y_\tau \to y_{\mu,e}$. The left panel of figure 7.1 shows that for Yukawa couplings y_l larger than y_τ we are in regime **b** where Y_B grows linearly with y_l. For smaller Yukawa couplings however, we are in regime **a**, where Y_B decreases as y_l^2. For equal values of the scale of new physics $\Lambda_e = \Lambda_\mu = \Lambda_\tau$ the values of Y_B in the electron and muon scenarios are then suppressed by a factor $(y_e/y_\tau)^2 \simeq 8 \cdot 10^{-8}$ and $(y_\mu/y_\tau)^2 \simeq 4 \cdot 10^{-3}$, respectively. For the electron, EDM constraints require $\Lambda_e > 5.7$ TeV, which suppresses the baryon asymmetry even more. The resulting values of Y_B are far below the observed asymmetries and we conclude that electron and muon CPV sources do not lead to successful baryogenesis.

7.4 Baryogenesis with a quark source

In this section we discuss baryogenesis with a quark CPV source and at first neglect the additional lepton-quark interaction introduced in section 7.2.6. We start the discussion with a CPV source in the top-quark sector. This scenario has been discussed extensively in the literature, see for example Refs. [282, 306, 340] where the same dimension-six CPV operator has been considered. Since the source is proportional to the value of the Yukawa coupling squared $S_f \propto y_f^2$, the baryon asymmetry generated by a top source can be expected to be larger than for the corresponding source terms

Approximation	FR(q)	N(q,t,h)	N(q,t,h,u)	N(q,t,h,u,l)	A(q,t,h,u,l)
Y_B	1.6×10^{-12}	3.5×10^{-13}	3.4×10^{-13}	1.5×10^{-12}	1.1×10^{-12}

TABLE 7.3: Baryon asymmetry Y_B for a top source using different approximations discussed in the main text. We used the benchmark values for the bubble-wall profile given in section 7.2.1 and $\Lambda_t = 7.1$ TeV consistent with EDM experiments.

involving lighter fermions. But several factors that were identified in section 7.2.5 suppress the corresponding BAU. We therefore study how effective a top source actually is. In the process we investigate the role of SM bottom and tau Yukawa interactions that are typically neglected.

A CPV bottom source is suppressed by $(y_b/y_t)^2 \simeq 4 \times 10^{-4}$ with respect to a top source. Part of this suppression can be compensated as EDM experiments do not set as stringent constraints on the CPV bottom source. In addition, a smaller Yukawa coupling also implies less washout because $\Gamma_M^{(b)}$ is smaller and, as demonstrated for a tau source, it is not immediately clear how Y_B varies with the size of the Yukawa coupling, and thus how the top and bottom scenarios compare. While the bottom Yukawa coupling is still roughly a factor two larger than the tau Yukawa coupling, we nevertheless expect the asymmetry to be suppressed with respect to the tau source, because the bottom has strong sphaleron interactions and a smaller diffusion constant leading to less efficient generation of Y_B.

7.4.1 Top source

We calculate the baryon asymmetry arising from a top CPV source using various approximations:

1. The simplest approximation is to first neglect the small bottom and tau Yukawa couplings. Using eqs. (5.31) and (5.37) leaves us with three transport equations for the number densities q, t, and h. Finally, we apply the often-used fast-rate approximation which assumes that the top Yukawa and strong sphaleron transitions are fast and (nearly) in equilibrium [252, 311]. This leaves us with a single equation for q that can be solved analytically. We denote the solution by FR(q).

2. We neglect bottom and tau Yukawa couplings, but do not use the fast-rate approximation. Instead we numerically solve the set of three transport equations for q, t, and h and call the solution N(q,t,h).

3. Next we include the effects of the bottom Yukawa. We can no longer connect the b density to those of light quarks and the transport equation for u has to be included. The numerical solution of the four transport equations is called $\mathrm{N}(q, t, h, u)$.

4. We also include the tau Yukawa coupling and add the l transport equation. In principle, we should keep the right-handed lepton fields too, but, as discussed in the tau scenario, the approximation of local lepton number conservation, $D_l = D_\tau$, is reasonable and we can eliminate the right-handed leptons. The solution is called $\mathrm{N}(q, t, h, u, l)$.

5. We solve the same set of equations using the semi-analytical method [312], which neglects the variation of the rates over the bubble wall, and write this solution as $\mathrm{A}(q, t, h, u, l)$.

As before between brackets in $A(...)$ and $N(...)$ we list the transport equations that we solve explicitly. The obtained values for Y_B for our benchmark point with $\Lambda_t = 7.1$ TeV and bubble-wall velocity $v_w = 0.05$ in the various approximations are listed in table 7.3. To get the right sign for Y_B, the sign of the CPV operator in eq. (7.1) is set to $s_t = 1$.

The fast-rate approximation assumes thermal equilibrium for the strong sphaleron and top Yukawa rates, but this approximation is invalid close to the bubble wall in the symmetric phase and invalid everywhere in the broken phase where $\Gamma_M^{(t)}$ is instead the fastest rate. By comparing the solutions $\mathrm{FR}(q)$ and $\mathrm{N}(q, t, h)$ we see that the fast-rate approximation overestimates Y_B by roughly a factor five and is thus a poor approximation, in agreement with the findings of Ref. [312]. The fast-rate approximation should be avoided to calculate Y_B, especially since it does not represent a systematic expansion and as such the associated error cannot be systematically estimated.

By comparing $\mathrm{N}(q, t, h)$ and $\mathrm{N}(q, t, h, u)$ we see that including bottom Yukawa interactions only provides a few-percent correction. Considering the significant intrinsic uncertainties associated to EWBG calculations, neglecting the bottom Yukawa seems a good approximation. It might come as a surprise then that including the even smaller tau Yukawa interaction has a much greater impact. The baryon asymmetry associated to $\mathrm{N}(q, t, h, u, l)$ is roughly five times that of $\mathrm{N}(q, t, h, u)$. Where does this lepton-induced enhancement stem from?

As discussed in section 7.2.5, when the strong sphaleron interactions are (approximately) in thermal equilibrium, $\mu_{\mathrm{ss}} \simeq 0$, the total chiral asymmetry in quarks is highly suppressed. This is illustrated in the left panel of figure 7.2. The red line depicts the chiral asymmetry in just top quarks, $q(z)$, as a function of the distance to the bubble wall in the symmetric phase. This individual asymmetry is everywhere much larger than the total chiral asymmetry in the quark sector, $n_L^{(q)}(z) \equiv \sum_i q_i$, where

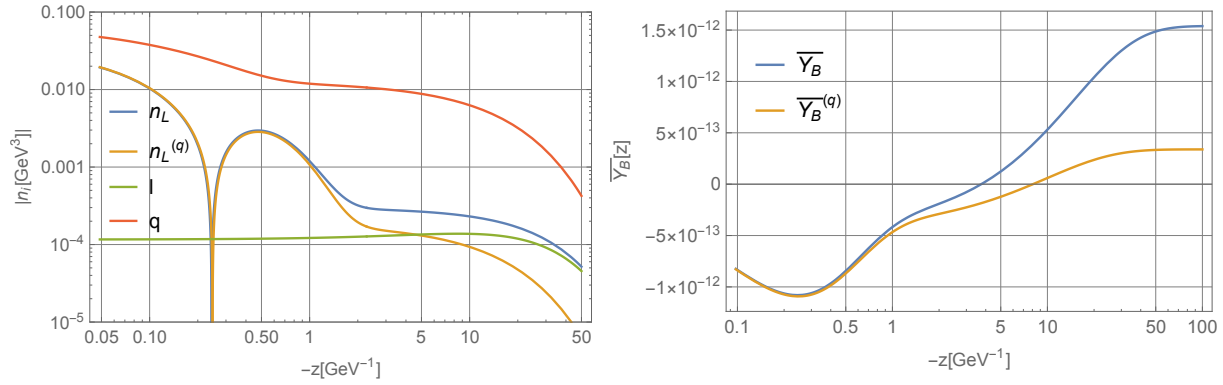

FIGURE 7.2: Left plot: absolute value of the number densities n_L, $n_L^{(q)}$, l, and q in the symmetric phase for a top source. The computation includes top, bottom and tau Yukawa interactions. Right plot: baryon asymmetry $\bar{Y}_B(z)$ and $\bar{Y}_B^{(q)}(z)$ as a function of the integration cut-off.

the sum runs over the three generations. $n_L^{(q)}(z)$ is plotted in orange and is itself larger than the chiral asymmetry in tau leptons, $l(z)$, depicted in green, up to $|z| \simeq 5\,\mathrm{GeV}^{-1}$. For larger distance $l(z)$ becomes larger and consequently dominates the total chiral asymmetry, $n_L(z) = n_L^{(q)}(z) + l(z)$, depicted in blue.

The distance from the bubble in the symmetric phase at which point the various densities start to drop can be understood qualitatively from the analytical solution for the lepton source discussed in the previous section. In analogy with the leptonic case there are three important length scales: the diffusion length $L^i_{\mathrm{diff}} \sim D_i/v_w$, the migration length set by strong sphaleron interactions $L_S^{(\mathrm{SS})} \sim \sqrt{k_q D_q/\Gamma_{\mathrm{ss}}} = \mathcal{O}(1)\,\mathrm{GeV}^{-1}$, and the migration length set by the top Yukawa interactions $L_S^{(y_t)} \sim \sqrt{k_q D_q/\Gamma_y^{(t)}} = \mathcal{O}(0.1)\,\mathrm{GeV}^{-1}$. The Yukawa interactions are strongest and provide the dominant source of washout near the bubble wall. This washout leads to the decrease of n_L for small values of z and the associated zero-crossing around $|z| = 0.2\,\mathrm{GeV}^{-1}$. At distances around $|z| \sim L_S^{(y_t)}$, the top Yukawa interactions are in equilibrium and the n_L would plateau to a constant value. However, this is not clear in figure 7.2 where n_L keeps decreasing because of washout from strong sphalerons which is active up to the larger distance $L_S^{(\mathrm{SS})}$. This washout, and the related decrease of n_L, ends for $|z| > L_S^{(\mathrm{SS})}$.

The individual particle densities migrate much further in the symmetric phase than the total quark chiral asymmetry, as their spread is only limited by diffusion. Indeed with both the top Yukawa and strong sphaleron interactions in equilibrium, the number densities of the left- and right-handed quarks and the Higgs are related (by the condition that the chemical potential vanishes). Physically what happens is that on the relevant time scales, quarks and Higgses are converted into each other

instantly, and they behave as a single degree of freedom that diffuses into the symmetric phase. Their diffusion length, which determines how far the densities extend, is dominated by the Higgs diffusion length which is large as the Higgs does not feel strong interactions. As such $L_{\rm diff} \sim D_h/v_w \simeq 20\,{\rm GeV}^{-1}$. A more precise estimate is obtained from the transport equation for the single degree of freedom, which gives (see eq. (77a) in Ref. [252]) $L_{\rm diff} \simeq 16\,{\rm GeV}^{-1}$.

Finally, the tau Yukawa interactions are out of equilibrium throughout. The lepton number density slightly increases away from the bubble wall as there is more time to convert Higgs quanta into leptons. The lepton asymmetry migrates over distances set by the lepton diffusion length $L_{\rm diff} \sim D_l/v_w \simeq 20\,{\rm GeV}^{-1}$. Because of the small tau Yukawa coupling the lepton density is always much smaller than the left-handed top density q. However, it is the chiral density that matters, and given the very efficient suppression of the chiral asymmetry in quarks, leptons actually start to dominate n_L for $|z| \gtrsim L_S^{(\rm SS)}$. This explains why the inclusion of leptons can give a sizeable correction to the final baryon asymmetry.

What is maybe surprising is that the leptons actually give the dominant contribution for our benchmark point. The reason for this is that $n_L^{(q)}$ crosses zero close to the bubble wall around $|z| = 0.25\,{\rm GeV}^{-1}$. In the right panel of figure 7.2 we show the contribution to the asymmetry from the wall up to a distance z. That is, we plot the function

$$\bar{Y}_B(z) = -\frac{3\Gamma_{\rm ws}}{2sD_q\alpha_+}\int_z^0 {\rm d}z'\, n_L(z'){\rm e}^{-\alpha_- z'}\,, \tag{7.24}$$

with $\alpha_\pm$ given in eq. (5.38). For our benchmark parameters, the chiral asymmetry close to the bubble wall $n_L \simeq n_L^{(q)}$ gives a negative contribution to the integral in eq. (5.38). However, past the zero-crossing the contribution becomes positive. Due to the sign change, the total asymmetry generated up to $z = 10\,{\rm GeV}^{-1}$ from just $n_L^{(q)}$ vanishes. Around this point, the chiral asymmetry in quarks is small and leptons dominate the chiral asymmetry. Integrating over larger distances, leptons then give the dominant contribution to Y_B. This sensitivity of Y_B to the tau Yukawa interactions is thus twofold: 1) even though small, they are the only mechanism via which the chiral asymmetry is transferred from the quark sector, where the CPV source is located, to the lepton sector, where they escape the efficient washout by strong sphalerons. 2) There is a cancellation of the contribution of $n_L^{(q)}$ to the baryon asymmetry.

We can now also understand why including bottom Yukawa interactions has less impact. These will transfer some of the top chiral asymmetry into a bottom chiral asymmetry, but the total is still

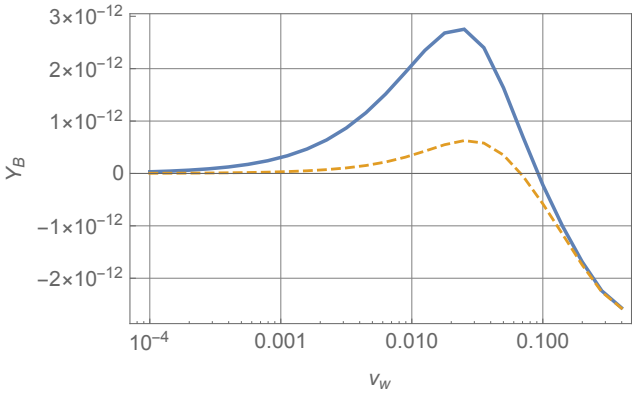

FIGURE 7.3: Y_B as a function of velocity v_w with (solid blue) and without (dashed orange) lepton interaction included.

washed out by strong sphaleron interactions. This transfer therefore does not lead to a significant change in Y_B.

An interesting question is now whether including tau leptons is generally important or whether it is a special feature of our benchmark parameters. To study this, we calculate Y_B associated to the $\mathrm{N}(q,t,h,u)$ and $\mathrm{N}(q,t,h,u,l)$ solutions for a wide range of bubble-wall velocities. The values of Y_B are plotted in figure 7.3. We conclude that the lepton contribution is important for a large range of velocities $v_w \sim 10^{-4} - 10^{-1}$, but becomes less relevant for larger velocities. For such large velocities the baryon asymmetry is dominated by the chiral asymmetry close to the bubble wall, where the leptons contribute little. In this case, the integral is cut off by the diffusion length $L_{\mathrm{diff}} \propto 1/v_w$, which becomes small.

7.4.2 Producing the universal baryon asymmetry with a top source

Let us finally answer whether a top source can produce the observed baryon asymmetry in eq. (5.1). For equal Wilson coefficients of the dimension-six CPV operators, $\Lambda_t = \Lambda_\tau$, the asymmetry induced by the top source is of the same order as for the tau source. However, for taus we can choose a fairly low scale $\Lambda_\tau \sim 1\,\mathrm{TeV}$, while EDM experiments constrain $\Lambda_t \geq 7.1$ TeV. As such, the asymmetry in our benchmark scenario is almost two orders of magnitude too small. As the asymmetry is rather sensitive to the Higgs vev at nucleation, this might be the easiest parameter to adjust to boost the asymmetry, but how much this is allowed depends on the details of the scalar sector that we have not specified. Our chosen bubble-wall velocity is already close to the optimal value as shown in figure 7.3. All things considered it seems unlikely that the dimension-six top Yukawa interaction can still lead to sufficient asymmetry.

Approximation	N(q,t,h,b)	N(q,t,h,b,l)	A(q,t,h,b)
Y_B	8.3×10^{-13}	8.4×10^{-13}	7.3×10^{-13}

TABLE 7.4: Baryon asymmetry Y_B for a bottom source with $\Lambda_b = 1\,\text{TeV}$ and $v_w = 0.05$ using different approximations discussed in the text.

It must be said, that the uncertainties in the calculation for a top CPV source are large. The vev-insertion approximation is dubious as the top Yukawa coupling is not small. We saw in section 5.3 that computing the top source in the semi-classical method of [266–268] leads to a source term that is about a factor 5 smaller. Another potentially large effect can be the inclusion of collective plasma effects, the so-called hole modes, in the calculation of the source term and interaction rates, see the discussion in Ref. [226]. Despite these caveats, it is fair to say that the observed baryon asymmetry is obtained more easily using a tau source, mainly due to the significant EDM constraints on the CPV top source. In section 7.5 we discuss ways of boosting the baryon asymmetry for top-source scenarios by adding additional BSM lepton-quark interactions. Other ways out could be by considering CP-violating interactions between top quarks and new scalar fields as such interactions are not directly constrained by EDMs if the new scalar field does not couple to electrons. Such a setup can appear in, for example, two-Higgs doublet models although several couplings have to be set to very small values by hand.

7.4.3 Bottom source

We now turn to the bottom source and investigate whether such a source can be as efficient as a tau source. To calculate the chiral asymmetry generated by a bottom source, one can use the same set of transport equations as for the top source. We calculate the asymmetry first by neglecting leptons and write this solution as $N(q,t,h,u)$. We then include tau Yukawa interactions and add the l-equation to the set of transport equations and obtain the solution $N(q,t,h,u,l)$. The corresponding semi-analytical solution is called A(q,t,h,u,l). The baryon asymmetry for our benchmark point with $\Lambda_b = 1\,\text{TeV}$ and bubble-wall velocity $v_w = 0.05$ is listed in table 7.4 (with $s_b = -1$ the sign of the dimension-six operator).

From the table it is clear that the asymmetry from a bottom source is almost two orders of magnitude smaller than the baryon asymmetry from a tau source for the same scale $\Lambda_b = \Lambda_\tau$. Just as for the top source, the chiral asymmetry in bottom quarks is effectively erased by the strong sphaleron interactions, which become important at $|z| \sim L_S^{(\text{SS})}$. Beyond this scale the leptons again give the dominant contribution to the chiral asymmetry, as can be seen in the left panel in figure 7.4.

However, unlike the top-source case, there is no zero-crossing, and thus no cancellation in Y_B. Now, the total baryon asymmetry is dominated by the contribution close to the bubble wall, where leptons are negligible, see the right panel in figure 7.4.

We conclude that the bottom source produces a value of Y_B that is about two orders of magnitude too small. What about sources involving even lighter quarks? In figure 7.5, the solid blue line depicts the value of Y_B as a function of the bottom Yukawa coupling y_b at the electroweak scale. The orange dashed line is a fit to a quadratic function of y_b. Effectively, for the SM value of y_b and smaller values we are in regime **a** discussed in section 7.3.3 where $Y_B \sim y_b^2$. Since the system of transport equations for an up, down, strange, or charm source is very similar to that of a bottom source, we expect that sources involving light quarks will be suppressed by $(y_q/y_b)^2$ compared to the numbers in table 7.4. Such sources will thus provide negligible contributions to Y_B. For $y_b \geq 0.04$ the asymmetry starts to scale linearly $Y_B \sim y_b$ (the system enters regime **b** discussed in section 7.3.3). The linear instead of quadratic scaling partially explains why a top source is not as effective compared to a bottom source as might be expected from just looking at the CPV source term.

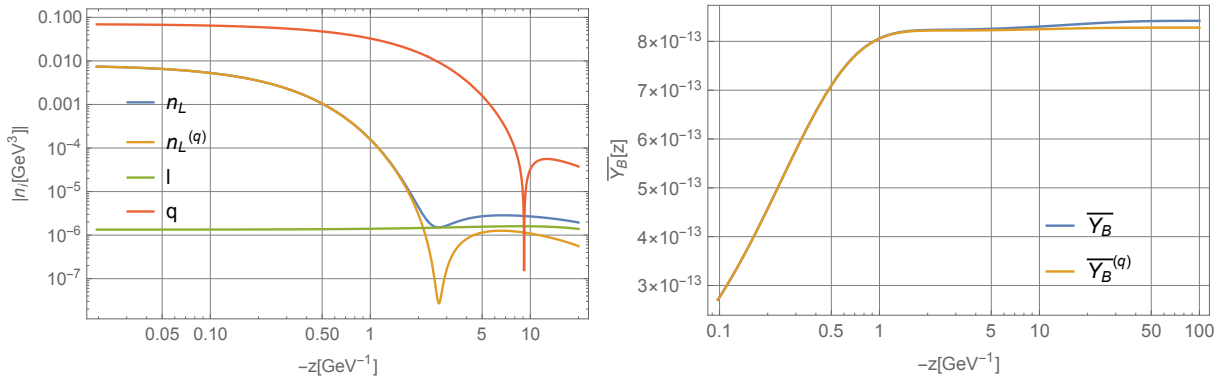

FIGURE 7.4: Left plot: absolute value of the number densities n_L, $n_L^{(q)}$, l and q in the symmetric phase for a bottom source. The computation includes top, bottom and tau Yukawa interactions. Right plot: baryon asymmetry $\bar{Y}_B(z)$ and $\bar{Y}_B^{(q)}$ as a function of the integration cut-off.

7.5 Consequences of additional quark-lepton interactions

In the previous sections we have argued that CP-violating leptonic sources are more effective than quark sources in generating a net baryon asymmetry. In this section, we analyze how we can modify the asymmetry by considering BSM interactions that transfer the chiral asymmetry from quarks into leptons (and vice versa). Such interactions can be induced in BSM models by the exchange of new particles such as additional scalar bosons or leptoquarks. In particular, we consider the

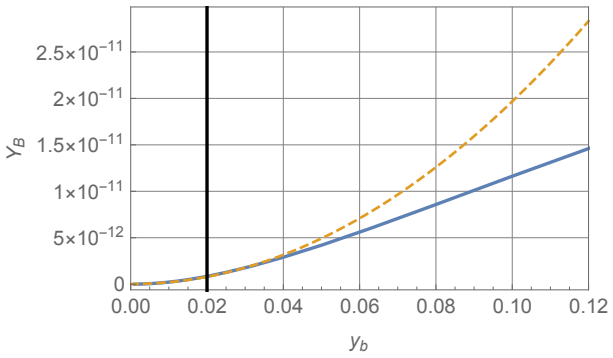

FIGURE 7.5: Baryon asymmetry for a bottom source as a function of the bottom Yukawa coupling y_b (solid blue line). The orange dashed line shows a quadratic fit and the black vertical line indicates the SM value of y_b at the electroweak scale.

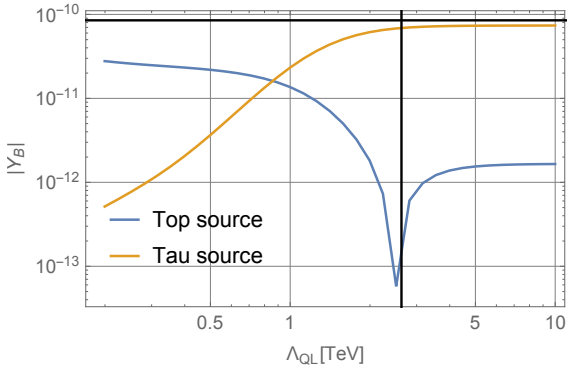

FIGURE 7.6: Y_B as function of $\Lambda_{\rm QL}$ for a top source with $\Lambda_t = 7.1 \times 10^3\,\text{GeV}$ (blue) and a lepton source with $\Lambda_\tau = 1 \times 10^3\,\text{GeV}$ (yellow). The vertical black line corresponds to the new interactions rate being equal to the lepton Yukawa interaction rate. The horizontal black line corresponds to the measured value of the baryon asymmetry.

effect of turning on a new top-tau coupling, which we parameterize by the dimension-six operator in eq. (7.13).

Intuitively, it is clear what to expect. For a top source, the chiral asymmetry in quarks is effectively washed out by the top Yukawa and especially by the strong sphaleron interactions. In such a scenario, any part of the chiral asymmetry that is transferred to the lepton sector survives this washout, and the more effectively this is done the larger the final baryon asymmetry. We thus expect an increase in Y_B for scales $\Lambda \lesssim 3\,\text{TeV}$ for which the new interaction rates becomes larger than the tau Yukawa interaction rate. For the lepton source scenario, we expect instead a decrease in the baryon asymmetry. The new interaction, if large, will transfer part of the chiral asymmetry from the lepton to the quark sector, where it is effectively washed out. This behavior is indeed borne out by our numerical simulations shown in figure 7.6, which shows the baryon asymmetry for a lepton (yellow line) and top-quark (blue line) source, for $\Lambda_\tau = 1\,\text{TeV}$ and $\Lambda_t = 7.1\,\text{TeV}$ consistent with experiment.

To obtain the observed baryon asymmetry eq. (5.1) with a top source requires a large top-lepton interaction, with a fairly low scale $\Lambda_{\rm QL} \lesssim 1\,\text{TeV}$ (as always, precise statements cannot be made due to significant theoretical uncertainties). To properly describe such a set-up probably requires going beyond the EFT description and adding the light degree of freedom that mediates the interaction. This might change the quantitative results, but we expect the results to be qualitatively the same. As the strength of the new coupling increases, the interactions approach equilibrium, and a further increase has limited effect; this explains the asymptotic flattening of Y_B for small cutoff $\Lambda_{\rm QL}$. The new coupling can boost the asymmetry by more than an order of magnitude. Naively one may have expected a $\mathcal{O}(10^2)$-increase, as the sphaleron washout reduces the chiral asymmetry in quarks by approximately this factor. However, even without the new interactions there is already transfer taking place via the SM Yukawa interactions. While the tau Yukawa is small, these effects already dominate the asymmetry for $\Lambda_{\rm QL} \to \infty$, as discussed in section 7.4.1.

While we considered here a top-tau interaction, the baryon asymmetry can also be boosted via additional interactions between top quarks and electrons or muons as the lepton flavor is irrelevant for the baryon asymmetry. The asymmetry can also be boosted by inclusion of BSM couplings between top and one of the lighter quarks. Such couplings, if sufficiently strong, would also avoid efficient washout by strong sphalerons, as discussed in section 7.2.6.

The effect of the dimension-six operator in eq. (7.13) in case of a lepton source is opposite as it now reduces the total asymmetry. As long as the new interactions are sufficiently suppressed $\Lambda_{\rm QL} \gtrsim 1\,\text{TeV}$, the chiral asymmetry stays mostly in the lepton sector and can be large enough to explain the observed value. However, for larger couplings the asymmetry can be suppressed by as much as two orders of magnitude. This effect can be seen in explicit models such as those studied in Refs. [326, 327] where a lepton CPV source is considered in the context of a two-Higgs doublet model. The source term, however, must be made rather large compared to the tau source discussed in section 7.3 (about a factor hundred larger) to generate a baryon asymmetry consistent with observations. The source originates from CPV Yukawa-interactions with heavier non-SM Higgs fields, which can be increased without running in conflict with experiments as long as the mixing angle between the heavier Higgs and the SM Higgs is sufficiently small. EDM bounds are also avoided by choosing couplings between the non-SM scalars and electrons and lighter quarks to be sufficiently small. The heavy scalars, however, lead to effective operators of the form of eq. (7.13) (although the actual lepton and quark flavor can vary) that, as shown in fig. 7.6, suppress the baryon asymmetry. As such, larger CPV sources are required. This example shows that the rather simple

framework considered here, based on effective operators can qualitatively describe the features of more complicated BSM models and can provide a useful guide in model building.

7.6 Discussion and conclusions

To satisfy the Sakharov conditions of CP-violation and out-of-equilibrium dynamics, many EWBG models have been proposed. In this chapter we do not commit to a specific model but instead apply EFT methods to describe the dynamics of EWBG. However, in chapter 6 we saw that EWBG cannot fully be embedded into the SM-EFT framework as a first-order phase transition requires additional light degrees of freedom that cannot be integrated out of the theory. In this chapter, we therefore describe the phase transition with a phenomenological ansatz and describe the required CPV with effective dimension-six operators containing SM fields only. Additional CPV operators involving the light degrees of freedom can certainly exist and be relevant, but as these are difficult to test experimentally, we leave them to future work.

We consider flavor-diagonal CPV dimension-six Yukawa operators of quarks and charged leptons with couplings that scale as y_f/Λ_f^2, where Λ_f is the scale where new physics appears and the EFT description breaks down. The resulting CPV source term that appears in the transport equation and drives the eventual generation of the baryon asymmetry scales as y_f^2/Λ_f^2. As such, for the same value of Λ_f it might be expected that the top quark would provide the largest baryon asymmetry. The recent electron EDM limit [297] sets a very strong constraint $\Lambda_t \geq 7.1$ TeV which ensures that a top CPV source as studied in this chapter cannot lead to the observed baryon asymmetry. For lighter fermions the CPV source term is suppressed by $(y_f/y_t)^2$, and even though the scale Λ_f is not as constrained, one might expect these light fermions to lead to even smaller asymmetries. We have investigated this in detail in this chapter and conclude that the naive scaling is not correct. Our main findings can be summarized as:

- Despite the Yukawa suppression, a CPV tau source leads to a baryon asymmetry of the same order of magnitude as induced by a top source for $\Lambda_\tau = \Lambda_t$. As EDM constraints on Λ_τ are much weaker, the tau source can produce the observed baryon asymmetry where a top source cannot. The relative effectiveness of the tau source with respect to the top source has several causes. While the top source is enhanced by $(y_t/y_\tau)^2$, the Yukawa and strong sphaleron rate effectively wash out a chiral asymmetry in top quarks. This washout is far less effective for tau leptons that have much smaller Yukawa couplings and do not participate in strong sphaleron

interactions. In addition, a chiral asymmetry in leptons diffuses much further into the plasma and electroweak sphaleron processes have more time to convert the chiral asymmetry into a baron asymmetry.

- We performed analytical and numerical calculations of varying sophistication of the baryon asymmetry in case of a tau CPV source. The analytical and numerical results are found to be in very good agreement. The analytical solutions provide insight into the dependence of the baryon asymmetry on parameters related to the phase transition, such as the bubble-wall velocity, and the size of the lepton Yukawa coupling. Depending on several parameters, we can identify regions where the baryon asymmetry scales as $\propto y_f^2$, as naively expected, but also as $\propto y_f$ showing explicit deviations from the naive scaling. As such, lighter fermions can be relatively effective in generating a baryon asymmetry.

- While tau leptons are more efficient than might be expected, our analytical solution shows that baryon asymmetries induced by muon or electron CPV dimension-six Yukawa interactions are suppressed by respectively $(y_\mu/y_\tau)^2$ and $(y_e/y_\tau)^2$. Such sources therefore lead to much too small baryon asymmetries and only the tau source is still phenomenologically relevant.

- Even in case of a top CPV source, leptons play an important role. The SM Yukawa interactions can convert a chiral asymmetry in quarks to a chiral asymmetry in leptons. This conversion is proportional to the tau Yukawa coupling and therefore often neglected. We find, however, that including tau leptons explicitly in the transport equations leads to a significant enhancement of the total baryon asymmetry up to an order of magnitude. This enhancement is a general feature over a wide range of bubble-wall velocities. We conclude that EWBG scenarios with CPV in the quark sector should explicitly include leptons in the transport equations. Despite this enhancement, the CPV top source from the dimension-six Yukawa interactions consistent with EDM experiments leads to a too small baryon asymmetry. This effectively rules out the minimal EWBG scenario of Ref. [278], although it must be stressed that the involved theoretical uncertainties are large.

- As a side result, we find that the fast-rate approximation which is often applied in studies of EWBG with CPV sources including top quarks, is not reliable. In our setup it significantly overestimates the total baryon asymmetry. This conclusion is in line with Ref. [312]. We recommend to avoid its use and to instead solve the complete set of transport equations.

- While the washout of the chiral asymmetry for a bottom CPV source is less effective than for a top CPV source, this does not compensate for the $(y_b/y_t)^2$ suppression of the CPV source.

We find that a CPV source from dimension-six bottom Yukawa interactions leads to a baryon asymmetry that is approximately two orders of magnitude smaller than a top CPV source for the same value $\Lambda_b = \Lambda_t$. For values of Λ_b consistent with EDM experiments this leads to a too small baryon asymmetry. For dimension-six Yukawa couplings for even lighter quarks the induced baryon asymmetries are even smaller.

- The total baryon asymmetry can be significantly altered in BSM models with more effective chiral-symmetry-breaking interactions between quarks and leptons than are present in the SM. In this chapter, we have modeled such interactions with effective dimension-six top-tau interactions that can be induced in explicit BSM models by the exchange of new particles. Such interactions can enhance, in case of a CPV quark source, or decrease, in case of a CPV lepton source, the baryon asymmetry by orders of magnitude. This mechanism can be useful to guide model building.

As a final remark, we would like to emphasize that although we looked at a specific implementation of CP violation via dimension-six Yukawa operators, our qualitative conclusions are more general. The importance of leptons and the related mechanism to boost the baryon asymmetry by transferring the chiral asymmetry from the quark to the lepton sector (or suppress it by doing the opposite), are independent of the details of our set-up.